Proceedings of the 11th ICPMG 2026
11th International Conference on Physical Modelling in Geotechnics
8-12 June 2026, Zurich, Switzerland

Pile Driving in Crushable Glauconite Sand Using X-ray Tomography

M.A. Sayyah
PhD Student, UGent Geotechnical Institute (UGGI), Ghent University, Ghent, Belgium, MohammadAmin.Sayyah@UGent.be

M.O. Ciantia
Senior Lecturer, School of Science and Engineering, University of Dundee, Dundee, United Kingdom
Associate professor, Department of Earth and Environmental Sciences, University of Milano-Bicocca, Milan, Italy, m.o.ciantia@dundee.ac.uk

M. Roustaei
Assistant professor, UGent Geotechnical Institute (UGGI), Ghent University, Ghent, Belgium, Mahya.Roustaei@UGent.be

ABSTRACT: Crushable sands such as calcareous and glauconitic deposits are widely encountered in offshore and coastal environments, particularly in continental shelves and shallow marine sediments. Unlike quartz sands, these materials are composed of weak, porous, and often biogenic or authigenic particles that are highly susceptible to grain crushing under installation-induced stresses. During offshore pile installation, high stress concentrations develop around the pile tip and along the shaft, promoting particle breakage, fabric collapse, and local densification. These processes can significantly alter the mechanical response of the soil, leading to nonlinear penetration resistance, changes in shaft friction, and post-installation reconsolidation effects. This study presents results from four physical pile driving tests using calcareous and glauconitic sands to assess the influence of sand type on pile penetration resistance and grain-scale degradation under controlled boundary conditions. Pile penetration resistance was continuously recorded during installation. X-ray computed tomography (XCT) scans were performed before and after pile driving. The results show that calcareous sand exhibits a more repeatable installation response, whereas glauconitic sand displays greater variability due to heterogeneous particle crushing and fabric evolution. XCT observations indicate that pile inclination develops in both materials, but its effect on lateral load mobilisation is more pronounced in glauconitic sand.

1 INTRODUCTION

Crushable sands are granular materials whose mechanical response is governed not only by particle rearrangement but also by stress-induced grain breakage, leading to irreversible changes in fabric, grading, stiffness, and permeability. Unlike quartz sands, crushable sands are typically composed of weak, porous, or friable minerals, such as biogenic carbonates or authigenic glauconite, which exhibit low crushing strength and high susceptibility to fragmentation under elevated stresses (Coop et al., 2004; Hardin, 1985; Marsal, 1967). Particle breakage in such materials significantly affects compressibility, shear strength, and critical state behaviour, and has been shown to play a dominant role in high-stress geotechnical applications, including pile installation and offshore foundations (Altuhafi et al., 2018; Bandini & Coop, 2011; Bolton, 1986).

Offshore and coastal environments frequently contain calcareous and glauconitic sands, particularly along continental shelves and shallow marine deposits. Calcareous sands, formed from biogenic debris such as coral fragments and shell remains, are characterized by angular particles, high intra-particle porosity, and low tensile strength, making them highly prone to crushing under installation loads (Folk, 1980; Scoffin, 1987; Shahnazari & Rezvani, 2013). Glauconitic sands consist of weak, iron-potassium phyllosilicate pellets that are mechanically fragile and susceptible to rapid degradation under compression and shear (Westgate et al., 2023). Previous studies have shown that while both materials are highly crushable, their breakage mechanisms differ: calcareous sands tend to exhibit localized fragmentation and rapid stiffness degradation, whereas glauconitic sands undergo progressive pellet collapse, fines generation, and a transition from sand-like to clay-like behaviour (Westgate et al., 2023; Zou et al., 2025).

Pile installation in crushable sands induces severe stress concentrations around the pile tip and along the shaft, triggering particle fragmentation, fabric collapse, and changes in load transfer mechanisms. Experimental and field investigations have demonstrated that particle breakage strongly influences pile penetration resistance, shaft friction mobilization, and post-installation reconsolidation behaviour (Altuhafi et al., 2018; Bandini & Coop, 2011; Yasufuku & Hyde, 1995). In offshore applications, these effects complicate pile drivability predictions and may lead to discrepancies between measured and predicted installation resistance when conventional design approaches, largely developed for non-crushable sands, are applied (Peng et al., 2024). In addition, breakage-induced fines generation and permeability reduction can affect excess pore pressure dissipation and long-term foundation performance under cyclic loading (Ovalle et al., 2015; Ovalle & Hicher, 2020).

Despite extensive laboratory research on particle breakage using triaxial, oedometer, and shear tests (Indraratna & Salim, 2002; Miao & Airey, 2013; Nakata et al., 2001), direct experimental evidence linking pile penetration behaviour to three-dimensional breakage patterns remains limited, particularly for glauconitic sands. Recent advances in X-ray computed tomography have enabled non-destructive visualization of internal soil structure and grain-scale damage (Alam et al., 2018; Karatza et al., 2019), yet most XCT studies focus on idealized loading paths rather than pile installation scenarios.

This study addresses this gap by presenting results from a series of physical pile driving tests conducted in calcareous and glauconitic sands, combined with pre- and post-installation XCT imaging.

2 MATERIAL AND METHOD

2.1 Tested Sands

Two natural crushable sands were investigated in this study: a calcareous sand and a glauconitic sand, selected to represent offshore-relevant materials with contrasting mineralogy and crushing behaviour.

The calcareous sand (Calc) was sourced from the Persian Gulf and is predominantly biogenic in origin. Mineralogical analyses indicate a calcium carbonate ($CaCO_3$) content of 92.2%, with the remaining 7.8% consisting of silicate minerals, including quartz, feldspars, mica, and biotite. The sand is composed of angular to sub-angular particles with high intra-particle porosity, making it highly susceptible to stress-induced crushing under pile installation loads.

The glauconitic sand (GL) was obtained from Antwerp, Belgium, a region where glauconite-rich deposits are commonly encountered in coastal and offshore environments. The material contains approximately 29% glauconite, primarily in the form of weak, rounded to sub-rounded pellets with high internal porosity. The remaining fraction consists of non-glauconitic sand-sized minerals. The mechanical fragility of glauconite pellets makes this sand particularly prone to progressive degradation and fines generation under loading.

Figure 1 presents the grain size distribution (GSD) curves of both materials prior to testing. The calcareous sand exhibits a coarser gradation with a wider particle size range, whereas the glauconitic sand is finer and more narrowly graded.

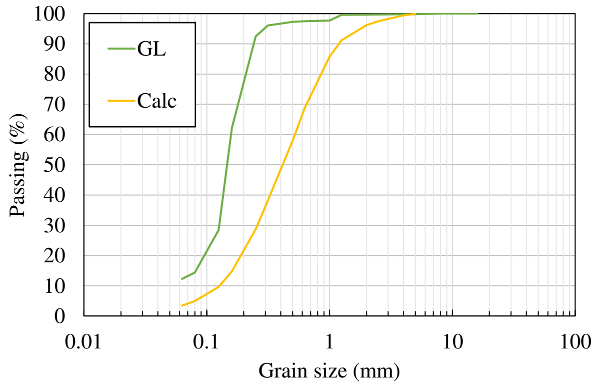

Figure 1. Initial grain size distribution of the calcareous (Calc) and glauconitic (GL) sands.

Photographs of the two sands in their initial state are shown in Figure 2, illustrating the clear differences in colour, texture, and apparent particle morphology.

Figure 2. Photographs of the calcareous (left) and glauconitic (right) sands prior to testing.

2.2 Experimental method

2.2.1 Loading frame

Pile driving tests were conducted in a transparent plexiglass cylindrical container with an internal diameter of 120 mm. The height of the sand specimen was approximately 160 mm, providing sufficient embedment length to investigate near-pile deformation while limiting boundary effects. Acrylic containers of similar dimensions have been widely adopted in small-scale pile installation studies to provide visual access and adequate confinement for mechanistic investigation of pile–soil interaction (Riccio, Ciantia, et al., 2024).

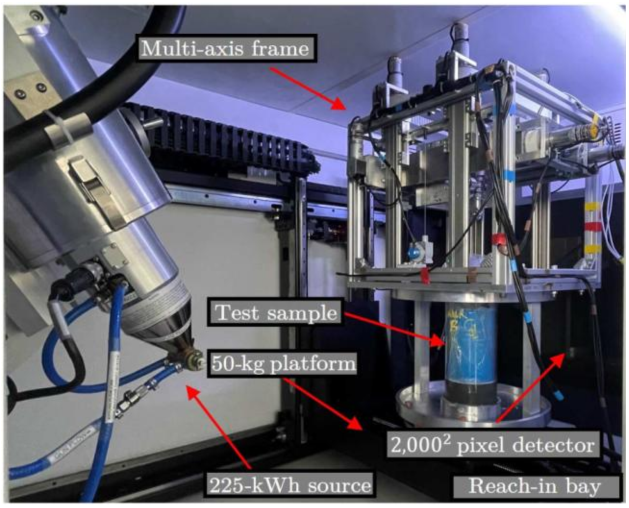

Figure 3. Multi-axis frame stationed in the University of Dundee Nikon XTH 225 CT scanner (Riccio, Ciantia, et al., 2024).

Pile installation was performed using a displacement-controlled loading frame developed at the University of Dundee for small-scale soil–structure interaction testing (Figure 3). The frame enables precise vertical displacement control and stable load application, allowing quasi-static pile installation under well-defined boundary conditions. Similar multi-axis and single-axis configurations have been successfully employed in previous experimental campaigns to study installation effects in sand and weak geomaterials, demonstrating the suitability of the system for grain-scale investigation of pile penetration mechanisms (Riccio, Romero, et al., 2024).

The reach-in bay is the shielded enclosure of the CT scanner where the test setup is positioned during scanning and loading. It houses the test sample, the rotating platform (with 50 kg load capacity), and the multi-axis loading frame within the chamber. The bay provides a controlled environment that allows X-ray imaging while ensuring operator safety from radiation exposure.

A solid wooden pile was installed vertically at the centre of the specimen. The diameter of the pile was 15mm. The pile was driven to a maximum penetration depth of 110 mm. Experimental and numerical studies show that most installation-induced stresses occur within $2 < r/R < 8$ from the pile axis, and decrease beyond this range (Yang et al., 2014). For the present pile (R = 7.5 mm), this corresponds to about 60 mm, which is equal to the container radius. Therefore, boundary effects are likely to be limited. Installation was carried out under quasi-static conditions, with a constant penetration rate selected to minimise inertial effects and allow progressive soil deformation. Based on penetration rates reported in the literature for small-scale pile installation in sand and weak geomaterials, a driving rate within the range of 0.2 mm/s was adopted (MA et al., 2024).

Penetration resistance was continuously recorded throughout installation. A total of 4 pile driving tests were performed: three in calcareous sand and two in glauconitic sand, each prepared at comparable initial conditions to enable direct comparison of material response.

2.2.2 Sample preparation

For each test, the plexiglass container was filled with dry sand in successive layers. The material was poured gently to minimise segregation and then lightly shaken by hand after filling to promote uniform packing while avoiding premature particle breakage during preparation.
The target bulk density was 1.43 g/cm³ for the calcareous sand and 1.47 g/cm³ for the glauconitic sand, corresponding to medium-dense states that were kept consistent across tests. After preparation, the specimen surface was levelled, and the pile was carefully aligned vertically prior to installation.

2.2.3 X-ray computed tomography (CT)

X-ray computed tomography was employed to characterise the internal soil structure before and after pile installation (Figure 3).

CT scans were acquired using a Nikon X-Tek system (Nikon Metrology NV). Image acquisition was performed using Inspect-X XT 6.12.1, and reconstruction was carried out with CT Agent XT 6.12.1. The reconstructed volumes consisted of 1631 × 2000 × 2000 voxels, corresponding to a physical volume of approximately 159 × 195 × 195 mm³. The voxel size was 0.097 mm in all three directions, yielding a total reconstructed volume of approximately 6.0×10^6 mm³.

3 RESULTS

3.1 Pile penetration resistance with depth

Figure 4 presents the evolution of pile penetration force with depth for the calcareous and glauconitic sands tested. Results are shown for two repeat tests in each material, enabling assessment of both material-dependent behaviour and test repeatability.

At shallow penetration depths (0–20 mm), all tests exhibit relatively low penetration resistance with comparable force levels. This initial stage corresponds to limited confinement near the surface, where soil displacement occurs under low overburden stress and particle rearrangement dominates the response. Minor fluctuations observed in this region are attributed to local fabric heterogeneity and initial pile–soil contact effects.

With increasing penetration depth, clear material-dependent trends emerge. In the calcareous sand, the penetration force increases gradually with depth, reaching moderate force levels at the final penetration depth. The two calcareous tests show similar overall trends, although local variations and small load drops are observed, particularly at intermediate depths (approximately 80 mm). These fluctuations are indicative of intermittent particle crushing and local fabric collapse, which are characteristic of highly crushable carbonate sands.

In contrast, the glauconitic sand exhibits a steeper increase in penetration resistance with depth. The penetration force rises more rapidly beyond approximately 40–50 mm, with one test (GL-test2) showing a pronounced increase in resistance toward the final penetration depth. The higher resistance and stronger depth dependency are consistent with progressive densification and degradation of weak glauconite pellets, leading to increased confinement and resistance ahead of the pile.

Despite some variability between repeat tests, the calcareous sand seems to show a relatively consistent penetration response, with both tests generally following similar force–depth trends and comparable resistance levels throughout installation. This could suggest a relatively stable installation behaviour under the tested density and boundary conditions. In contrast, the glauconitic sand may exhibit a more complex and variable response, with noticeable differences between the two repeat tests despite identical material composition and initial density. This variability might be related to local fabric rearrangement, possible crushing of weak glauconite pellets, and changes in confinement conditions that can influence the penetration behaviour during loading. Overall, these observations may indicate that glauconitic sand could be somewhat more sensitive to installation-induced disturbance than calcareous sand under the tested conditions..

3.2 Lateral pile load during installation

Figure 5 presents the evolution of the lateral (horizontal) pile load with depth during installation for the calcareous and glauconitic sands. Lateral loads were measured in two orthogonal horizontal directions, perpendicular to each other, in order to capture any asymmetric force development associated with pile inclination. For clarity, the figure reports the maximum lateral load recorded at each penetration depth from the two measurement directions.

Although the magnitude of the lateral load is small compared to the axial penetration force, measurable horizontal forces develop progressively with depth. The lateral load is associated with the observed pile inclination during installation. This inclination was confirmed by post-installation CT observations, where a deviation of the pile axis from the vertical can be identified. Despite the small tilt angle, the increasing confinement of the surrounding soil with depth results in the mobilisation of appreciable lateral forces, particularly at larger penetration depths.

Material-dependent differences can be observed. The calcareous sand appears to exhibit a relatively stable and repeatable lateral load response, with both tests generally following similar trends throughout installation. In contrast, the glauconitic sand may show a more complex and variable behaviour, with noticeable differences between repeat tests despite identical material composition and initial density. This variability could be associated with the sensitivity of glauconitic sand to local fabric evolution and possible particle crushing, which may influence lateral force transfer during installation.

3.3 X-ray computed tomography observations

Figure 6 presents selected post-installation XCT slices for the calcareous and glauconitic sand tests, illustrating the final pile position and the surrounding soil structure after installation. In both materials, the XCT images reveal a measurable pile inclination, which developed during installation. It should be noted that a slight initial misalignment at the pile head or small imperfections in vertical positioning may have contributed to the onset of this inclination. The subsequent evolution of tilt during penetration reflects the interaction between the pile and the surrounding soil.

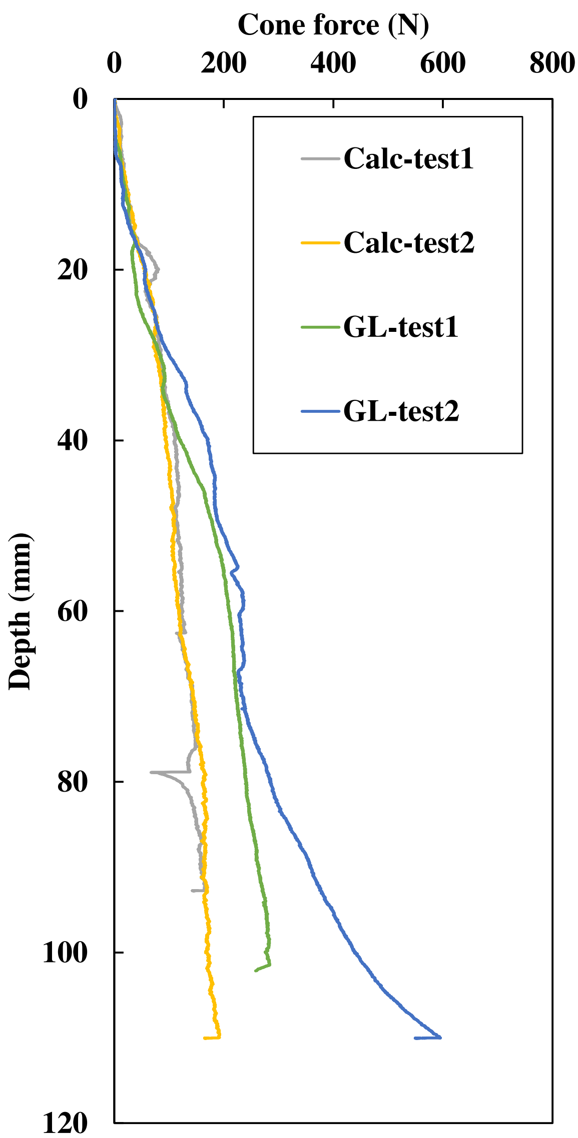

Figure 4. Pile penetration force versus depth in calcareous and glauconitic sands.

In the calcareous sand, inclination angles of 12.38° (Calc-test1) and 3.37° (Calc-test2) were measured. Although structural changes are expected to occur in highly crushable carbonate sands under installation stresses, the present XCT data do not allow direct quantification of particle breakage or fabric evolution. The post-installation images suggest that the soil structure surrounding the pile appears relatively symmetric in both tests. Consequently, despite the presence of pile tilt, its influence on the lateral load response appears to remain relatively moderate, and both tests generally exhibit stable and repeatable mechanical behavior. In the glauconitic sand, inclination angles of 2.67° (GL-test1) and 6.24° (GL-test2) were observed. While the absolute tilt angles are broadly comparable to those measured in the calcareous sand, their mechanical consequences may differ. The XCT images suggest spatial variations in soil structure around the pile, which could reflect material-dependent deformation processes during installation. As a result, the pile inclination in glauconitic sand may be associated with greater variation in the lateral load response.

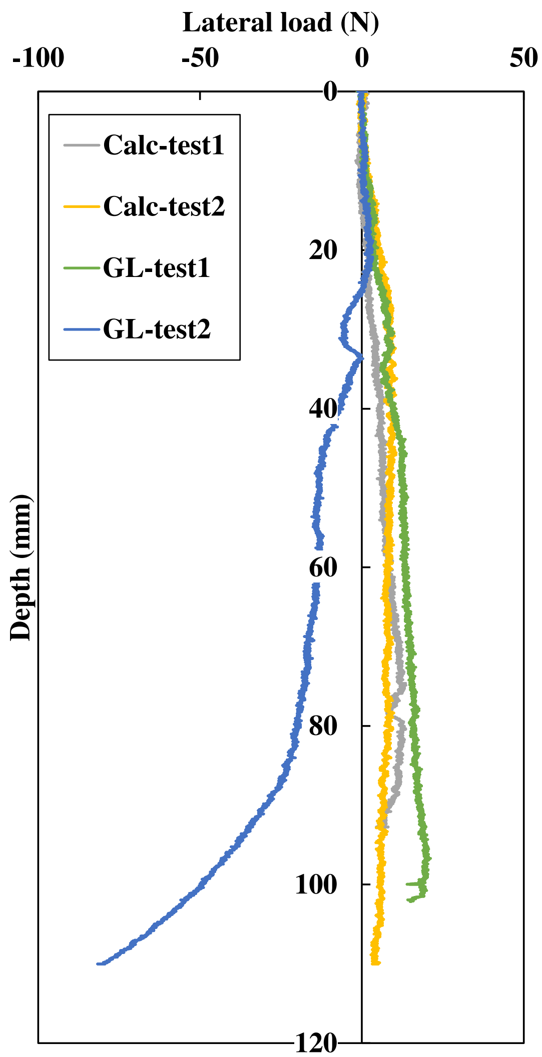

Figure 5. Maximum lateral load versus depth during pile installation in calcareous and glauconitic sands.

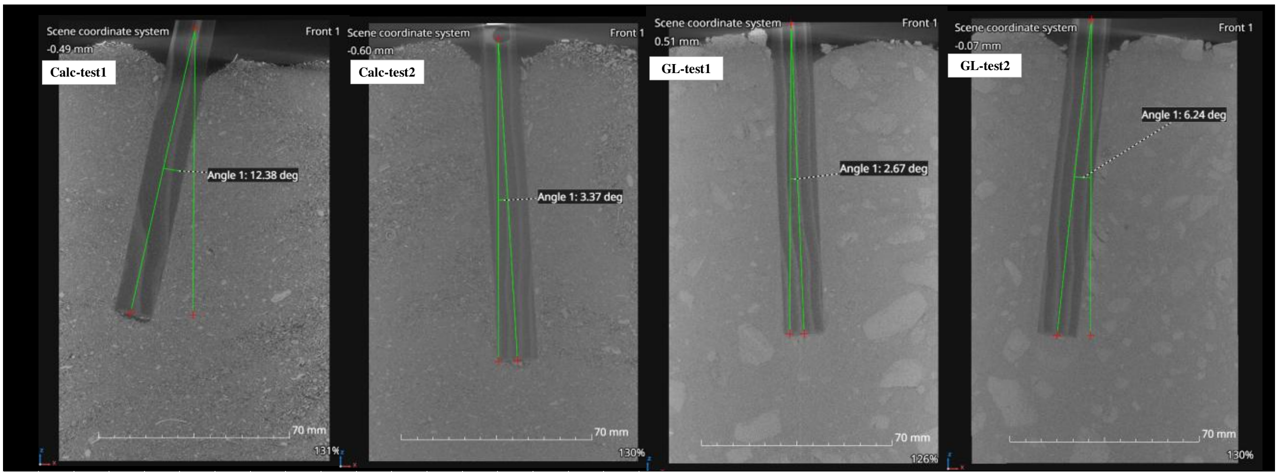

Figure 6. Post-installation XCT slices showing pile inclination in calcareous and glauconitic sands.

This effect can be observed when comparing GL-test1 and GL-test2, where an increase in pile tilt is accompanied by a noticeable increase and redistribution of lateral load during installation. This contrast may indicate that, in glauconitic sand, relatively small differences in pile inclination can be associated with differences in lateral force mobilization.

Overall, these observations suggest that pile inclination can develop in both sands during installation. While crushable materials such as calcareous and glauconitic sands may be susceptible to particle damage under elevated stresses, the present experimental results mainly indicate a correlation between pile inclination and lateral load response rather than a direct causal link with grain-scale crushing mechanisms. Further quantitative investigation would be needed to clearly establish the micromechanical origin of the observed behavior.

4 CONCLUSION

This study investigated pile installation behaviour in crushable calcareous and glauconitic sands using small-scale physical modelling combined with pre- and post-installation X-ray computed tomography. The results suggest that calcareous sand may exhibit a more repeatable penetration response, whereas glauconitic sand can show greater variability in both penetration and lateral load behaviour under comparable initial conditions. XCT observations indicate that pile inclination can develop in both materials during installation, and its mechanical influence on lateral load mobilisation may be more noticeable in glauconitic sand. Although crushable sands may undergo particle damage under installation stresses, the voxel size used in the present scans (0.097 mm) is not sufficient to directly resolve grain-scale breakage or fines generation. Therefore, the findings mainly indicate a correlation between pile inclination and lateral load response rather than a direct causal link with micromechanical crushing mechanisms. The results highlight the potential importance of material-dependent structural response in pile–soil interaction and suggest that higher-resolution imaging would be required to explicitly relate macroscopic installation behaviour to particle breakage processes.

5 ACKNOWLEDGMENT

The authors gratefully acknowledge that the experimental data presented in this study were collected during tests conducted at the University of Dundee under the supervision of Dr. Matteo Oryem Ciantia. The authors sincerely thank Dr. Wei Wang (Postdoctoral Researcher) for his valuable technical assistance during the experimental program. X-ray computed tomography scanning was performed at the SMART Laboratory, University of Dundee, with the expert support of Dr. Laszlo Csetenyi, whose assistance is greatly appreciated. Financial support for the research visit to the United Kingdom was provided by the Research Foundation – Flanders (FWO) through the mobility grant V432225N, which is gratefully acknowledged.

6 REFERENCE

Alam, M. F., Haque, A., & Ranjith, P. G. (2018). A study of the particle-level fabric and morphology of granular soils under one-dimensional compression using insitu X-ray CT imaging. *Materials*, *11*(6), 919.

Altuhafi, F. N., Jardine, R. J., Georgiannou, V. N., & Moinet, W. W. (2018). Effects of particle breakage and stress reversal on the behaviour of sand around displacement piles. *Géotechnique*, *68*(6), 546–555. https://doi.org/10.1680/jgeot.17.P.117

Bandini, V., & Coop, M. R. (2011). The Influence of Particle Breakage on the Location of the Critical State Line of Sands. *Soils and Foundations*, *51*(4), 591–600. https://doi.org/10.3208/sandf.51.591

Bolton, M. (1986). The strength and dilatancy of sands. *Geotechnique*, *36*(1), 65–78.

Coop, M. R., Sorensen, K. K., Bodas Freitas, T., & Georgoutsos, G. (2004). Particle breakage during shearing of a carbonate sand. *Géotechnique*, *54*(3), 157–163. https://doi.org/10.1680/geot.2004.54.3.157

Folk, R. L. (1980). *Petrology of sedimentary rocks*. Hemphill publishing company.

Hardin, B. O. (1985). Crushing of Soil Particles. *Journal of Geotechnical Engineering*, *111*(10), 1177–1192. https://doi.org/10.1061/(ASCE)0733-9410(1985)111:10(1177)

Indraratna, B., & Salim, W. (2002). Modelling of particle breakage of coarse aggregates incorporating strength and dilatancy. *Proceedings of the Institution of Civil Engineers-Geotechnical Engineering*, *155*(4), 243–252.

Karatza, Z., Andò, E., Papanicolopulos, S.-A., Viggiani, G., & Ooi, J. Y. (2019). Effect of particle morphology and contacts on particle breakage in a granular assembly studied using X-ray tomography. *Granular Matter*, *21*(3), 44. https://doi.org/10.1007/s10035-019-0898-2

MA, D., HAN, X., CAI, Z., & GUAN, Y. (2024). Numerical analysis of earth pressure distribution law on pile shaft of displacement pile. *Rock and Soil Mechanics*, *45*(6), 1863–1872.

Marsal, R. J. (1967). Large Scale Testing of Rockfill Materials. *Journal of the Soil Mechanics and Foundations Division*, *93*(2), 27–43. https://doi.org/10.1061/JSFEAQ.0000958

Miao, G., & Airey, D. (2013). Breakage and ultimate states for a carbonate sand. *Géotechnique*, *63*(14), 1221–1229. https://doi.org/10.1680/geot.12.P.111

Nakata, Y., Kato, Y., Hyodo, M., Hyde, A. F., & Murata, H. (2001). One-dimensional compression behaviour of uniformly graded sand related to single particle crushing strength. *Soils and Foundations*, *41*(2), 39–51.

Ovalle, C., Dano, C., Hicher, P.-Y., & Cisternas, M. (2015). Experimental framework for evaluating the mechanical behavior of dry and wet crushable granular materials based on the particle breakage ratio. *Canadian Geotechnical Journal*, *52*(5), 587–598. https://doi.org/10.1139/cgj-2014-0079

Ovalle, C., & Hicher, P.-Y. (2020). Modeling the effect of wetting on the mechanical behavior of crushable granular materials. *Geoscience Frontiers*, *11*(2), 487–494. https://doi.org/10.1016/j.gsf.2019.06.009

Peng, Y., Yin, Z.-Y., Yang, F., Qu, L., & Ding, X. (2024). Analysis of the effect of breakable particle corners on uplift pile–soil interaction behaviors in calcareous sand. *Acta Geotechnica*, *19*(11), 7307–7328. https://doi.org/10.1007/s11440-024-02367-z

Riccio, T., Ciantia, M. O., Previtali, M., Brown, M. J., & Csetenyi, L. (2024). A 4D investigation of model pile installation. In *Geotechnical Engineering Challenges to Meet Current and Emerging Needs of Society* (pp. 3270–3273). CRC Press.

Riccio, T., Romero, T., Previtali, M., Mánica, M., & Ciantia, M. (2024). A 4D Soil-Structure Interaction Model Testing Apparatus. *Geotechnical Testing Journal*, *47*(6), 1181–1204. https://doi.org/10.1520/GTJ20230581

Scoffin, T. P. (1987). *Introduction to carbonate sediments and rocks*.

Shahnazari, H., & Rezvani, R. (2013). Effective parameters for the particle breakage of calcareous sands: An experimental study. *Engineering Geology*, *159*, 98–105. https://doi.org/10.1016/j.enggeo.2013.03.005

Westgate, Z. J., DeGroot, D. J., McMullin, C., Zou, Y., Guo, D., Van Haren, S., Beemer, R. D., Zeppilli, D., Miller, K. G., & Browning, J. V. (2023). Effect of degradation on geotechnical behavior of glauconite sands from the U.S. Mid-Atlantic Coastal Plain. *Ocean Engineering*, *283*. https://doi.org/10.1016/j.oceaneng.2023.115081

Yang, Z. X., Jardine, R. J., Zhu, B. T., & Rimoy, S. (2014). Stresses Developed around Displacement Piles Penetration in Sand. *Journal of Geotechnical and Geoenvironmental Engineering*, *140*(3), 04013027. https://doi.org/10.1061/(ASCE)GT.1943-5606.0001022

Yasufuku, N., & Hyde, A. F. L. (1995). Pile end-bearing capacity in crushable sands. *Géotechnique*, *45*(4), 663–676. https://doi.org/10.1680/geot.1995.45.4.663

Zou, Y., DeGroot, D. J., & Westgate, Z. J. (2025). Direct and Interface Shear Behavior of an Authigenic Glauconite Sand from the Coastal Plain of New Jersey. *Journal of Geotechnical and Geoenvironmental Engineering*, *151*(7), 04025065.